NANO LETTERS

LETTER

pubs.acs.org/NanoLett

Benzenedithiol: A Broad-Range Single-Channel Molecular Conductor

Youngsang Kim,[†] Torsten Pietsch,[†] Artur Erbe,[‡] Wolfgang Belzig,[†] and Elke Scheer*[,†]

[†]Department of Physics, University of Konstanz, 78457 Konstanz, Germany

[‡]Helmholtz-Zentrum Dresden Rossendorf, 01328 Dresden, Germany

Supporting Information

ABSTRACT: More than a decade after the first report of single-molecule conductance, it remains a challenging goal to prove the exact nature of the transport through single molecules, including the number of transport channels and the origin of these channels from a molecular orbital point of view. We demonstrate for the archetypical organic molecule, benzenedithiol (BDT), incorporated into a mechanically controllable break junction at low temperature, how this information can be deduced from studies of the elastic and inelastic current contributions. We are able to tune the molecular conformation and thus the transport properties by displacing the nanogap electrodes. We observe stable contacts with low conductance in the order of 10^{-3} conductance quanta as well as with high conductance values above ~0.5 quanta. Our observations show unambiguously that the conductance of BDT is carried by a single transport channel provided by the same molecular level, which is coupled to the metallic electrodes, through the whole conductance range. This makes BDT particularly interesting for applications as a broad range coherent molecular conductor with tunable conductance.

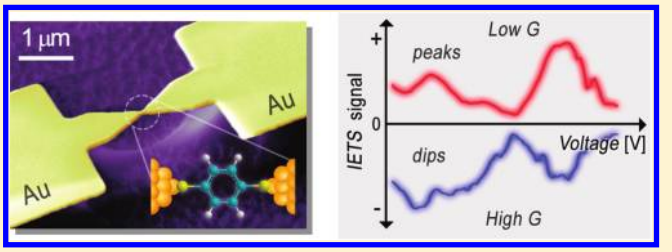

KEYWORDS: Single molecule, break junction, inelastic electron tunneling spectroscopy, benzenedithiol, single-level model

The number and the transmission probabilities of the current-carrying modes yield important information for understanding the nature of the charge transport through molecular junctions. Hydrogen molecules contacted by platinum electrodes accommodate a single and perfectly transmitting transport channel as demonstrated in the seminal experiment of Smit et al. by shot-noise and inelastic electron transport studies.[1] For applications of single-molecule junctions in more complex electronic circuits, hydrogen is not suitable, because it is too small and volatile. A molecule providing tunable conductance in a rather broad range while keeping the advantages of a single-transport channel would therefore be desirable. The conductance of single-molecule junctions can routinely be tuned by adjusting the distance between two electrodes using mechanically controlled break-junction (MCBJ) or scanning tunnel microscope (STM) techniques.[2−15] For example, 1,4-benzenedithiol (BDT) molecules, as a conjugated molecule with one aromatic ring, are reported to show a variable conductance ranging from $\sim 10^{-4} G_0$ to $\sim 0.5 G_0$, with the quantum of conductance $G_0 = 2e^2/h$.[13−18] Such large variation occur because the BDT molecule may adopt several conformations in the junction when the molecular junction is stretched or compressed. These includes a tilting of the ring plane with respect to the electrodes or bonding to different sites on the metal atoms (i.e., top or hollow).[13−19] This makes BDT a very promising candidate for studying fundamental aspects of quantum transport and also for manifold applications in molecular electronics devices, provided that the configuration and conformation can be controlled. Recently, the single-level model has been found to successfully describe the charge transport through such conjugated molecules.[20,21] In this model the conduction channel is formed by the coupling of a molecular orbital to the Fermi sea of the electrodes and its conductance is described by a transmission function $T(E,V)$ (see below). A change of configuration affects the molecular level position (E_0), the level broadening (Γ), or both and thus influences the conductance and the shape of the current−voltage ($I-V$) characteristics. The contribution of inelastic transport processes, i.e., induced by electron-vibration (vibronic) coupling, varies in the different conductance regimes (high or low conductance), because their contribution to the current is determined by the transmission of the junction.[7,22−26] The influence of vibronic coupling onto the conductance of molecular junctions is most easily examined by means of inelastic electron tunneling spectroscopy (IETS).[7,22−28] The IETS measurement is sensitive to the molecular conformation (or orientation), contact geometry, and electrode−molecule coupling.[8,9,12,28,29] The excitation of vibrational modes of the molecular junction is possible when the bias voltage exceeds the energy of the vibrational mode ($eV \geq \pm\hbar\omega$, where ω is the frequency of the vibrational mode). In the low conductance regime the possibility of inelastic charge transport results in an enhanced probability of forward scattering.[7,22−25] However, in the range of higher transmission the electron backscattering increases due to a momentum transfer to the excited mode, leading to a negative

Received: May 25, 2011
Revised: July 19, 2011
Published: August 01, 2011

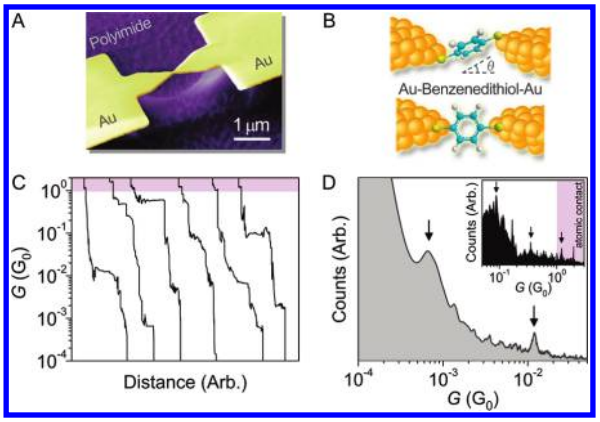

Figure 1. (A) Scanning electron microscopy image of the MCBJ device. (B) Illustrations of an Au−BDT−Au junction: top, the tilt angle (θ) of the benzene ring with respect to the current path; bottom, the binding of sulfur (S) at the hollow site of Au atom sites. (C) The conductance traces of BDT molecular junctions are shown for the opening process. The shaded area is metallic contact region. (D) Conductance histograms of BDT molecular junctions. The histogram is collected by repeating the opening and closing process 300 times. The arrows indicate the prominent conductance peaks of the histograms. The inset is the histogram at higher conductance regime including the metallic contact regime (shaded area).

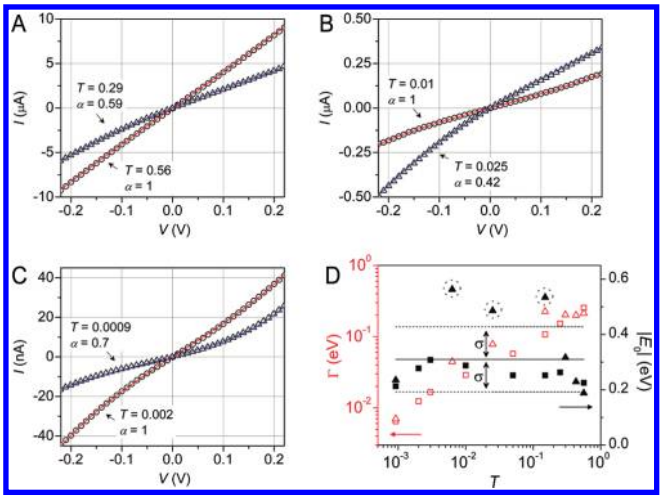

Figure 2. (A−C) The symmetric (circle) and asymmetric (triangle) $I-V$ curves of BDT molecular junctions at different transmission regimes are fitted using the Landauer formula (solid line, red and blue) in the voltage range ±0.22 V. (a) The best-fit parameters are $\Gamma = 253 \pm 8$ meV, $|E_0| = 225 \pm 8$ meV for $T = 0.56$ and $\alpha = 1$; $\Gamma_R = 75 \pm 1$ meV, $\Gamma_L = 127 \pm 4$ meV, $|E_0| = 317 \pm 6$ meV for $T = 0.29$ and $\alpha = 0.59$. (b) $\Gamma = 29 \pm 0.3$ meV, $|E_0| = 288 \pm 3$ meV for $T = 0.01$ and $\alpha = 1$; $\Gamma_R = 23 \pm 0.3$ meV, $\Gamma_L = 55 \pm 2$ meV, $|E_0| = 486 \pm 10$ meV for $T = 0.025$ and $\alpha = 0.42$. (c) $\Gamma = 12 \pm 0.3$ meV, $|E_0| = 278 \pm 5$ meV for $T = 0.002$ and $\alpha = 1$; $\Gamma_R = 4 \pm 0.04$ meV, $\Gamma_L = 2.8 \pm 0.02$ meV, $|E_0| = 225 \pm 1$ meV for $T = 0.0009$ and $\alpha = 0.7$. (d) The level broadening ($\Gamma = \Gamma_R + \Gamma_L$, left side, red, open symbols) and the position of the molecular level ($|E_0|$, right side, black, filled symbols) are obtained by fitting the $I-V$ curves in a wide range of transmission (T). The square and triangle symbols indicate the symmetric and asymmetric coupling, respectively. Solid and dashed lines indicate the average (0.31 eV) and standard deviation ($\sigma = \pm 0.12$ eV) values of all $|E_0|$, respectively. Dotted circle is marked to indicate the strong asymmetric coupling ($\alpha < 0.5$).

contribution (or reduction) of the transmission probability.[7,22−25] Hence, in the tunneling regime (low conductance) the inelastic excitations appear as *peaks* in the second derivative of the $I-V$ characteristics, corresponding to *enhanced* differential conductance above this threshold voltage.[7−9,12,22−28] In contrast to that, the excitation of vibrational modes gives rise to *dips* in the IETS, i.e., a *reduced* differential conductance, when the transmission (T) exceeds the so-called crossover transmission ($T_{crossover}$), which is given by half the value of the maximum transmission (T_{max}) of a junction, where T is the transmission in the linear conductance regime.[7,22−26] The transition between both regimes has not been reported experimentally for prototypical organic molecules, such as BDT.

In this article, we report charge transport measurements through single BDT molecules connecting Au electrodes using the low-temperature MCBJ technique. IETS measurements are carried out in a wide range of transmission regimes, and reveal a pronounced amplitude variation and sign of the vibronic contributions. The level broadening Γ and molecular level position E_0 are examined as a function of the transmission using the single-level model. The quantitative findings indicate that the charge transport in BDT single-molecule junctions is carried by a single dominant channel provided by the same molecular orbital.

A scanning electron microscope image of a nanofabricated device is shown in Figure 1A. A sketch of a single BDT molecule bridging the Au electrodes by the MCBJ technique is illustrated in Figure 1B. Detailed sample fabrication is given in the Supporting Information. Charge transport measurements through BDT molecules were carried out in a custom-designed cryogenic vacuum insert equipped with a MCBJ system; all transport measurements are performed at 4.2 K (see Supporting Information for details of the measurement setup).[9,28] To determine the preferential conductance of Au−BDT−Au junctions, we repeatedly opened and closed the junctions; typical conductance traces of the BDT molecular junctions are in the range of $1G_0$ and $10^{-4}G_0$ in Figure 1C. The mean stretching length of the molecular junction is obtained as ∼8.4 Å (see Supporting Information). This length is defined as the stretching length after breaking the metallic Au−Au contact until the breaking of the metal−molecule contact. The beginning and the end of the stretching length are included by the conductance falling abruptly below $1G_0$ and $10^{-4}G_0$, respectively. The molecular length of BDT between the sulfur terminated groups was estimated to be 6.47 Å using the CambridgeSoft Chem3D (see Supporting Information).

The conductance histogram was measured to identify the most prominent conductance values as shown in Figure 1D. The multiple conductance peaks can be attributed to both the change of contact geometry[9,11] and molecular orientation.[14,15,18,19] The lowest dominant conductance value (the error range is defined by the half width at half-maximum (HWHM) in the histogram) was found at $((6.6 \pm 5.2) \times 10^{-4})G_0$, in agreement with previously reported studies.[3,30] This indicates an entirely straight metal−molecule−metal junction. (The sulfur (S) end groups may bind on top of Au atoms on both electrodes.) The highest conductance peak ($\sim 0.5G_0$) is less well pronounced. However, there is a finite probability to obtain such highly conductive molecular junctions. They are often interpreted as arising either from an almost perpendicularly orientated benzene ring (tilt angle $\theta \sim \pi/2$) or by the binding of the S end group at the hollow site of Au, as illustrated in Figure 1B.[13−15,18,19] It was predicted theoretically that changing the tilt angle from $\theta = 0$ to 70° increases the

dx.doi.org/10.1021/nl201777m |Nano Lett. 2011, 11, 3734–3738

conductance by a factor of ~33 from $(\sim 1.5 \times 10^{-3})G_0$ to $(\sim 5 \times 10^{-2})G_0$ for the benzenedithiol molecule.[18] Moreover the larger tilt angle of benzenedithiol in combination with the binding at the hollow site was also reported to contribute significantly to the enhancement of conductance above $\sim 0.5G_0$.[14]

To elucidate this phenomenon, we consider the influence of molecular level (E_0) and level broadening (Γ) of the transmission $T(E,V)$. The molecular level ($|E_0| = E_F - E_{HOMO}$, HOMO indicates the highest occupied molecular orbital, the transport through Au−BDT−Au junctions is known to be dominated by the HOMO level.[27,31]) and the level broadening ($\Gamma = \Gamma_R + \Gamma_L$, where Γ_R and Γ_L denote the coupling constants to the right and the left lead, respectively) are obtained in a broad conductance range by fitting the $I-V$ curves using the Landauer formula[2,20,21]

$$I(V) = \frac{2e}{h}\int_{-\infty}^{\infty} T(E,V)[f(E - eV/2) - f(E + eV/2)]\,dE \quad (1)$$

where e is electron charge, h is Planck's constant, and $f(E)$ is the Fermi−Dirac distribution function. The transmission function $T(E,V)$ and the energy level $E_0(V)$ are expressed as

$$T(E,V) = \frac{4\Gamma_L\Gamma_R}{[E - E_0(V)]^2 + [\Gamma_L + \Gamma_R]^2} \quad (2)$$

$$E_0(V) = E_0 + \left(\frac{\Gamma_L - \Gamma_R}{\Gamma_L + \Gamma_R}\right)\frac{eV}{2} \quad (3)$$

Here we assume that the current-carrying molecular level shifts, when a bias voltage is applied, according to the asymmetry of the coupling strength to the leads. Both the $I-V$ and the fitting curves are presented in panels A−C of Figure 2 for symmetric ($\alpha = 1$) and asymmetric ($\alpha \neq 1$) couplings, respectively. The degree of coupling asymmetry is defined by $\alpha = \Gamma_R/\Gamma_L$ or Γ_L/Γ_R (with the bigger of both values in the denominator, $\alpha = 1$ indicates the symmetric coupling). The linear conductance is related to the transmission via $G = TG_0 = T(V{=}0)G_0$. The calculated level broadening (Γ) and the energy level (E_0) are displayed in Figure 2D. In principle these two parameters (Γ and E_0) may change simultaneously, leading to a variation of the transmission of the metal−molecule−metal junctions. Interestingly, for Au−BDT−Au we observe that the level broadening depends on the transmission, whereas the energy of the molecular level does not. In other words, the conductance and its development upon changing the electrode distance are mainly determined by the level broadening defined by the electrode−molecule coupling. We assume that the strength of the electrode−molecule coupling is influenced by both the tilt angle of the BDT molecule and the binding of the end group on top or hollow site, supported by previous theoretical studies.[18,21] An average value with standard deviation for the molecular level of $|E_0| = 0.31 \pm 0.12$ eV is obtained for both symmetric and asymmetric coupling of Au−BDT−Au junctions. This value is consistent with both experimental[3,32] and the recent theoretical studies.[33] As shown in Figure 2D, the molecular level $|E_0|$ adopts values in two different regions. The three data points (in the dotted circle) are significantly higher than the others. Such large values of $|E_0| \sim 0.5$ eV appear for strongly asymmetric coupling when α is lower than 0.5 and can have several origins. The first assumption that the shift of the effective level $E_0(V)$ is completely defined by the ratio of the transport coupling strength (eq 3) may be trivial. In particular for weak coupling with strong asymmetry, charging effects may have to be included. In this asymmetric weak coupling regime, a description via capacitive coupling (with capacitances C_L and C_R to the left and the right electrode) might be more appropriate. However, this would add two more free parameters, which cannot be determined independently in our measurements. In the second scenario, the shift of $E_0(V)$ can be very pronounced, such that another orbital is the closest to E_F and therefore would dominate the charge transport. The fact that E_0 changes between two well-defined values is in favor of this latter option. Measurements of the thermopower could clarify this question.[31,34]

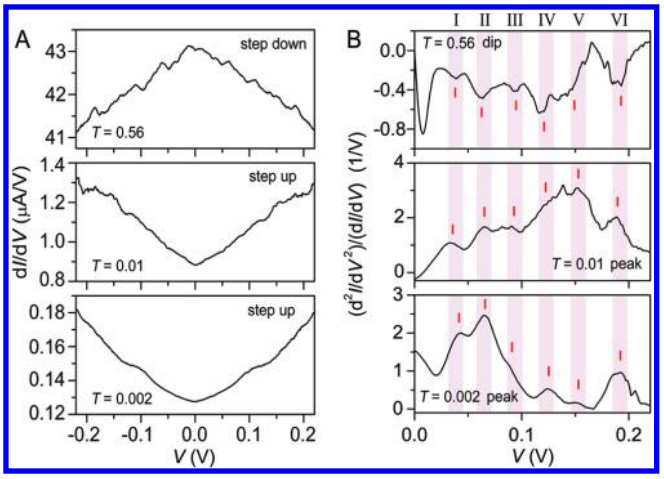

Figure 3. (A) Differential conductance (dI/dV) curves are obtained as a function of bias voltage for a contact with $T = 0.56$ (top panel), 0.01 (mid panel), and 0.002 (bottom panel). The conductance steps downward at $T > \sim 0.5$, whereas it steps upward for $T < \sim 0.5$. (B) Normalized IETSs measured for the contact with $T = 0.56$ (top panel), 0.01 (mid panel), and 0.002 (bottom panel) is presented. Likewise the IETS spectra change their sign from dips to peaks. The vibrational modes of Au−BDT−Au junctions are assigned: I, gold−sulfur stretching (ν(Au−S)); II, C−S stretching (ν(C−S)); III, C−C−C bending (γ(C−C−C)); IV, C−H in-plain stretching (ν(C−H)); V, C−H in-plain bending (γ(C−H)); VI, C═C stretching (ν(C═C)). The vertical dashes indicate the maximum dip or peak of each vibrational mode. The detailed assignments are presented in Table 1 of the Supporting Information.

In the various transmission regimes, differential conductance (dI/dV) and the IETS measurements are performed in a diverse range of transmissions to scrutinize the effect of the transmission on the vibronic coupling as shown in panels A and B of Figure 3. The symmetric dI/dV and IETS curves of Au−BDT−Au junctions measured at $T = 0.56$, 0.01, and 0.002 were obtained from a stepwise opening process of an individual sample. In Figure 3B the IETS (d^2I/dV^2) is normalized with the dI/dV in order to compensate for the conductance change, and hence the IETS amplitude is defined as $(d^2I/dV^2)/(dI/dV)$.[9,12,27,28]

Well-pronounced features (dips or peaks of the IETS amplitude) occur at voltages corresponding to the energy of molecular vibrations. The details of the assignment of these features to vibrational modes (labeled as I to VI in Figure 3B) are explained in the caption of Figure 3B and Table S1 of the Supporting Information. Although the voltages, at which the features occur, are comparable for all junctions, their sign is not.

dx.doi.org/10.1021/nl201777m |Nano Lett. 2011, 11, 3734–3738

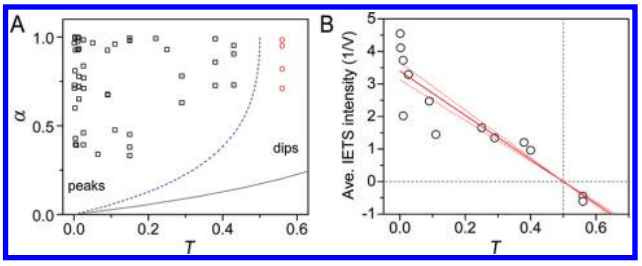

Figure 4. (A) The changes of peaks (square, black) and dips (circle, red) for different degrees of coupling asymmetry (α) are displayed as a function of the transmission (T). The parameter α is obtained from the fitting of $I-V$ curves, and the peaks and dips are evaluated from IETS spectra. The dashed line delimits the crossover transmission ($T_{crossover}$), and the solid line indicates the maximum transmission (T_{max}). (B) The average normalized intensities $(d^2I/dV^2)/(dI/dV)$ (averaged over the six assigned modes labeled I to VI) for the symmetrically coupled junctions are displayed as a function of the transmission (T). The intensity of IETS follows the linear relation (solid line) of $1-2T$. Dashed lines indicate the error range of the linear regression.

The symmetric dI/dV in Figure 3A obtained at $T = 0.56$ shows a reduced conductance at the threshold voltages corresponding to molecular vibrational modes, while the IETS in Figure 3B shows dips at the same transmission. However, at $T = 0.01$ and 0.002, the dI/dV and IETS are stepwise enhanced and show peaks rather than dips. The latter observation corresponds to the expected behavior for transmissions below $T_{crossover}$, while the first one is expected for $T > T_{crossover}$.

High transmission with 0.56 could be achieved via the contributions of several molecules in parallel or by direct Au−Au contacts. However, larger contacts with contributions from several molecules in parallel, summing up to a total transmission of 0.56, should show peaks in IETS as expected for low-transmission junctions. On the other hand, metallic Au−Au contacts would not excite the molecular vibrational modes. The IETS spectrum of the junction, which shows dips, with $T = 0.56$ proves that this very high conductance state of the Au−BDT−Au junctions is indeed realized by a single molecule with robust Au−S bonds. The sign change of IETS has been observed before in simple molecules as, e.g., water (H_2O), in which the transport through a single and highly conductive transport channel is expected.[7] The fact that the expected sign change occurs for the π-conjugated organic molecule (i.e., BDT) again suggests that the transport through this molecule is dominated by a single channel, even in the high-transmission regime $T > \sim 0.5$. As we mentioned above, the existence of a single channel allows us to use the conductance (G/G_0) synonymously with the transmission (T).

The crossover transmission ($T_{crossover}$) in the single-level model, which separates the transmission range between a dip and a peak of IETS, is given by $T_{crossover} = T_{max}/2$. The maximum transmission (T_{max}) depends on the degree of coupling asymmetry, $T_{max} = 4\alpha/(1 + \alpha)^2$.[22−25] The relevant energy level of organic molecules, might it be the HOMO or the LUMO, is in general located too far away to align with the Fermi level (E_F) of the electrodes by the applied voltage; i.e., the transport is in the off-resonant tunneling regime and gives rise to low transmission. However, for the Au−BDT−Au junction a maximum transmission (T_{max}) of ∼1 has been predicted given by a molecular state forming close to E_F,[14,15] and the crossover transmission becomes 0.5 in the case of $\alpha = 1$ (symmetric coupling).[22−25] For the asymmetric coupling, $T_{crossover}$ is lower. In Figure 4A the contacts revealing peaks and dips as a function of transmission and asymmetry are shown. The degree of coupling asymmetry is defined by fitting the $I-V$ curves using eq 1. According to our data the crossover regime is between $T = 0.56$ and 0.42 for the case of symmetric coupling. Also for asymmetric coupling all our observations are consistent with the expected behavior of the single-level model, indicating again that the tunneling process through the Au−BDT−Au junction is dominated by one transmission channel.[22−25]

Finally we discuss the dependence of the normalized IETS intensity $(d^2I/dV^2)/(dI/dV)$ on the transmission as shown in Figure 4B for the case of symmetric coupling ($\alpha = 1$). We determine the peak intensities of all vibrational modes (six modes labeled as I−VI in Figure 3B) measured in one transmission regime by using the normalized amplitude values without subtraction of any background signal. These values are averaged, and then the averaged intensity is plotted as a function of the transmission. Since at $T_{crossover}$ the intensity is zero, it increases positively or negatively at lower or higher transmission, respectively.[23,25] For a single-channel contact, the normalized intensity is predicted to depend linearly on the transmission according to $1-2T$, in perfect agreement with our observation.[23]

In conclusion, we performed $I-V$, dI/dV, and IETS measurements for Au−1,4-benzenedithiol−Au single-molecule junctions at 4.2 K while controling the nanogap of single-molecule junctions. We were able to form stable molecular junctions in a broad range of transmission from $T = 0.002$ to 0.56. The high transmission regime can only be accessed when the electrode coupling is sufficiently strong. In our experiment this is achieved by pushing the two metal electrodes together. By tuning the transmission probability and studying the differential conductance and the IETS, we observed the contributions of vibronic excitations on the charge transport. The crossover between dips and peaks of IETS is evaluated to be in the range $T \sim 0.42-0.56$ for the case of symmetric coupling. Moreover, we showed for the first time that not only the energy position of the vibronic excitations can be analyzed but also the normalized IETS intensity obeys the predicted relation of $1-2T$. The analysis of the $I-V$ measurements revealed that the level broadening determines the transmission, while the energy of the current-carrying orbital is rather independent of the coupling and the transmission. Although this combined analysis does not present a rigorous determination of the number and the transmission of the conduction channels, it suggests that the charge carriers tunnel via a single dominant channel, also in the high transmission state ($T > \sim 0.5$) of the BDT molecular junction. Therefore, BDT is one of the very rare organic molecules which are able to span the range from low transmission to high transmission; thus it is very useful for molecular electronics applications as well as a testbed for addressing fundamental questions of quantum transport in molecules.

■ ASSOCIATED CONTENT

Ⓢ Supporting Information. Details on experimental procedures, vibrational mode assignment, and stretching distance of molecular junctions. This material is available free of charge via the Internet at http://pubs.acs.org.

■ AUTHOR INFORMATION

Corresponding Author
*E-mail: elke.scheer@uni-konstanz.de.

■ ACKNOWLEDGMENT

We thank Fabian Pauly, Federica Haupt, Juan Carlos Cuevas, and Yi Luo for fruitful discussion. This work was supported by the Deutsche Forschungsgemeinschaft through SFB767 and Priority Program SPP 1243.

■ REFERENCES

(1) Smit, R. H. M.; Noat, Y.; Untiedt, C.; Lang, N. D.; van Hemert, M. C.; van Ruitenbeek, J. M. *Nature* **2002**, *419*, 906–909.
(2) Cuevas, J. C.; Scheer, E. *Molecular Electronics—An Introduction to Theory and Experiment*; World Scientific Publishing: Singapore, 2010.
(3) Reed, M. A.; Zhou, C.; Muller, C. J.; Burgin, T. P.; Tour, J. M. *Science* **1997**, *278*, 252–254.
(4) Nitzan, A.; Ratner, M. A. *Science* **2003**, *300*, 1384–1389.
(5) Champagne, A. R.; Pasupathy, A. N.; Ralph, D. C. *Nano Lett.* **2005**, *5*, 305–308.
(6) Venkataraman, L.; Klare, J. E.; Nuckolls, C.; Hybertsen, M. S.; Steigerwal, M. L. *Nature* **2006**, *442*, 904–907.
(7) Tal, O.; Krieger, M.; Leerink, B.; van Ruitenbeek, J. M. *Phys. Rev. Lett.* **2008**, *100*, 196804.
(8) Paulsson, M.; Krag, C.; Frederiksen, T.; Brandbyge, M. *Nano Lett.* **2009**, *9*, 117–121.
(9) Kim, Y.; Song, H.; Strigl, F.; Pernau, H.-F.; Lee, T.; Scheer, E. *Phys. Rev. Lett.* **2011**, *106*, 196804.
(10) Li, X.; He, J.; Hihath, J.; Xu, B.; Lindsay, S. M.; Tao, N. *J. Am. Chem. Soc.* **2006**, *128*, 2135–2141.
(11) Li, C.; Pobelov, I.; Wandlowski, T.; Bagrets, A.; Arnold, A.; Evers, F. *J. Am. Chem. Soc.* **2008**, *130*, 318–326.
(12) Arroyo, C. R.; Frederiksen, T.; Rubio-Bollinger, G.; Vélez, M.; Arnau, A.; Sánchez-Portal, D.; Agraït, N. *Phys. Rev. B* **2010**, *81*, 075405.
(13) Tsutsui, M.; Teramae, Y.; Kurokawa, S.; Sakai, A. *Appl. Phys. Lett.* **2006**, *89*, 163111.
(14) Sergueev, N.; Tsetseris, L.; Varga, K.; Pantelides, S. *Phys. Rev. B* **2010**, *82*, 073106.
(15) Pontes, R. B.; Rocha, A. R.; Sanvito, S.; Fazzio, A.; da Silva, A. J. R. *ACS Nano* **2011**, *5*, 795–804.
(16) Martin, C. A.; Ding, D.; van der Zant, H. S.; van Ruitenbeek, J. M. *New J. Phys.* **2008**, *10*, 065008.
(17) Taniguchi, M.; Tsutsui, M.; Yokota, K.; Kawai, T. *Nanotechnology* **2009**, *20*, 434008.
(18) Haiss, W.; Wang, C.; Jitchati, R.; Grace, I.; Martín, S.; Batsanov, A. S.; Higgins, S. J.; Bryce, M. R.; Lambert, C. J.; Jensen, P. S.; Nichols, R. J. *J. Phys.: Condens. Matter* **2008**, *20*, 374119.
(19) Bratkovsky, A. M.; Kornilovitch, P. E. *Phys. Rev. B* **2003**, *67*, 115307.
(20) Huisman, E. H.; Guédon, C. M.; van Wees, B. J.; van der Molen, S. J. *Nano Lett.* **2009**, *9*, 3909–3913.
(21) Zotti, L. A.; Kirchner, T.; Cuevas, J.-C.; Pauly, F.; Huhn, T.; Scheer, E.; Erbe, A. *Small* **2010**, *6*, 1529–1535.
(22) Paulsson, M.; Frederiksen, T.; Ueba, H.; Lorente, N.; Brandbyge, M. *Phys. Rev. Lett.* **2008**, *100*, 226604.
(23) de la Vega, L.; Martín-Rodero, A.; Agraït, N.; Yeyati, A. L. *Phys. Rev. B* **2006**, *73*, 075428.
(24) Shimazaki, T.; Asai, Y. *Phys. Rev. B* **2008**, *77*, 115428.
(25) Frederiksen, T.; Lorente, N.; Paulsson, M.; Brandbyge, M. *Phys. Rev. B* **2007**, *75*, 235441.
(26) Böhler, T.; Edtbauer, A.; Scheer, E. *New J. Phys.* **2009**, *11*, 013036.
(27) Song, H.; Kim, Y.; Jang, Y. H.; Jeong, H.; Reed, M. A.; Lee, T. *Nature* **2009**, *462*, 1039–1043.
(28) Kim, Y.; Hellmuth, T. J.; Bürkle, M.; Pauly, F.; Scheer, E. *ACS Nano* **2011**, *5*, 4104–4111.
(29) Lin, L.-L.; Wang, C.-K.; Luo, Y. *ACS Nano* **2011**, *5*, 2257–2263.
(30) Ghosh, S.; Halimun, H.; Mahapatro, A. K.; Choi, J.; Lodha, S.; Janes, D. *Appl. Phys. Lett.* **2005**, *87*, 233509.
(31) Reddy, P.; Jang, S.-Y.; Segalman, R. A.; Majumdar, A. *Science* **2007**, *315*, 1568.
(32) Lörtscher, E.; Weber, H. B.; Riel, H. *Phys. Rev. Lett.* **2007**, *98*, 176807.
(33) Strange, M.; Rostgaard, C.; Häkkinen, H.; Thygesen, K. S. *Phys. Rev. B* **2011**, *83*, 115108.
(34) Pauly, F.; Viljas, J. K.; Cuevas, J. C. *Phys. Rev. B* **2008**, *78*, 035315.